Front. Optoelectron. 2020, 13(3): 235–245
https://doi.org/10.1007/s12200-020-1042-y

REVIEW ARTICLE

# Focus on performance of perovskite light-emitting diodes

**Peipei DU[1], Liang GAO[2], Jiang TANG (✉)[2]**

1 State Key Laboratory of Material Processing and Die and Mould Technology, School of Materials Science and Engineering, Huazhong University of Science and Technology, Wuhan 430074, China
2 Wuhan National Laboratory for Optoelectronics and School of Optical and Electronic Information, Huazhong University of Science and Technology, Wuhan 430074, China



**Abstract** Perovskite-based optoelectronic devices, especially perovskite light-emitting diodes (PeLEDs) and perovskite solar cells, have recently attracted considerable attention. The National Renewable Energy Laboratory (NREL) chart inspires us to develop a counterpart for PeLEDs. In this study, we collect the record performance of PeLEDs including several new entries to address their latest external quantum efficiency (EQE), highest luminance, and stability status. We hope that these performance tables and future updated versions will show the frontiers of PeLEDs, assist researchers in capturing the overview of this field, identify the remaining challenges, and predict the promising research directions.

**Keywords** metal halide perovskite, light-emitting diode (LED), performance table

## 1 Introduction

Metal halide perovskites, a class of promising semiconductor materials with superior photoelectric properties, have produced a significant progress in solar cells, light-emitting diodes (LEDs), photodetectors, and lasers [1]. Thus far, the most active research area is solar cells, which enjoy a continually improved efficiency and growing commercial activities. Their efficiency evolution is available on the National Renewable Energy Laboratory (NREL) chart, which records the best certified efficiencies of state-of-the-art solar cells from 1976 to the present day. This chart allows readers to conveniently track industry trends and cutting-edge research status, which accelerates the advancement of this field.

However, until now, there has been no record line, chart, or even a review for perovskite light-emitting diodes (PeLEDs). In 2018, Cao et al. [2] and Lin et al. [3] have simultaneously reported highly efficient near-infrared and green PeLEDs with an external quantum efficiency (EQE) greater than 20%. The EQEs of PeLEDs matched those of commercial organic LEDs (OLEDs) in approximately four years after their development [4], which suggests the unparalleled potential of PeLEDs in lighting and display applications. Soon after, a red PeLED with an EQE of 21.6% was developed [5], which marked 2018 as a milestone in the development of PeLEDs. In addition, efficient blue PeLEDs have been recently reported [6,7]. Encouraged by the unprecedentedly rapid progress [8], more researchers have focused on PeLEDs and produced many encouraging results.

In this paper, we present useful tables containing world-class PeLEDs, aiming to provide researchers working on PeLED technologies with a valuable information resource. In addition, some performance tables summarize the core parameters of PeLEDs with the best EQE, record luminance, and noteworthy operation lifetime. Moreover, PeLEDs, which are based on lead-free materials and new manufacturing processes, are separately collected to exploit additional benefits. These tables will be renewed with the further progress of this field to provide additional support for researchers. Thus, this study reviews the present status and outlines the future trends of PeLED research.

## 2 Criterion for statistics

All data in the following figures and tables are extracted from reported studies that were published before April 2020. Of note, standard certification for LEDs has not been adopted to evaluate the performance of PeLEDs [9]. Herein, peak EQE is used to rank the PeLED efficiency regardless of the errors between different measurement

Received April 27, 2020; accepted May 15, 2020

E-mail: jtang@mail.hust.edu.cn

systems. For the operation stability, superior devices and competitive cases are shown despite different test conditions. A compromised rule is developed to distinguish the emission color of PeLEDs as follows: electroluminescence (EL) peak shorter than 500 nm is blue, 510–540 nm is green, 630–700 nm is red, and beyond 750 nm is near-infrared.

## 3 Performance tables

Classified according to the EL peak, Table 1 lists the best-performing PeLEDs in different emission bands. The columns include color, perovskite composition, dimensionality, EL peak, device structure, EQE, maximum luminance ($L_{max}$), current efficiency, stability, active area, full width at half maximum (FWHM), CIE coordinate, note, and publication date. We attempted to make this table current and comprehensive by recording all notable studies on solution-processed lead-based PeLEDs. In addition, special cases are also recorded such as optical out-coupling enhancement. The stability and luminance records are separately noted irrespective of the EQE value.

Of note, perovskites in Table 1 are all fabricated by spin coating, which is facile for manufacturing in a laboratory. We insist that vacuum deposition also shows considerable advantages in perovskite film processing (e.g., absence of solubility limit, good reproducibility with uniform morphology, and scaled-up production [10]), which makes it a competitive fabrication technique for the potential commercialization of PeLEDs. Table 2 lists several PeLEDs produced by vacuum methods, which include thermal evaporation (co-evaporation or layer-by-layer deposition), chemical vapor deposition (CVD), and vacuum-assisted multi-deposition. There is only one report on vacuum-deposited blue or red PeLEDs; more attention is dedicated to green PeLEDs. After approximately three years, the EQEs of vacuum-fabricated LEDs gradually exceeded 4%; however, these values are still considerably lower than those of solution-processed PeLEDs.

Finally, Table 3 shows lead-free LEDs to demonstrate environmentally friendly candidates without the toxic heavy metal. Only several studies incorporated lead-free perovskites or perovskite derivatives into LEDs, with the best EQE of 3.8%. However, there have been many lead-free materials with good photoluminescence properties reported in the literature [46–50], which enables further EQE and luminance improvement of lead-free LEDs. In addition, the FWHM of lead-free PeLEDs is several times wider than that of lead-based PeLEDs, which make them more suitable for lighting instead of display applications.

After compiling the performance of state-of-the-art PeLEDs, we further subdivide perovskite categories into three parts by dimensionality (Fig. 1). From the material point of view, dimensionality engineering has been widely adopted. Low-dimensional perovskites with a larger exciton binding energy show enhanced radiative recombination and higher EQE [62]. Therefore, we summarized the highest EQEs (Fig. 1(a)) and luminance (Fig. 1(b)) of bulk, quasi-two-dimensional (quasi-2D), and quantum dot (QD) PeLEDs with conventional device architectures apart from out-coupling strategies.

## 4 What lies behind the statistics

**Metal halide perovskites possess considerable potential in LED applications.** The EQEs of green, red, and near-infrared PeLEDs have reached over 20%, which is comparable to those of commercial OLEDs. In addition, the FWHM of PeLEDs is narrower than that of OLEDs, which indicates a more saturated color gamut in the National Television System Committee (NTSC) standard. This rapid and exciting progress attracts and encourages more researchers toward this rising field, as indicated by the upsurge in published papers in this field. With more institutions and researchers delving into this field, the performance, stability, and manufacturability of PeLEDs can be hopefully pushed to surpass those of OLEDs in the near future, which enables their display and lighting applications.

**Operation stability is the major existing challenge.** The reported lifetime of PeLEDs lags far behind that of OLEDs and QLEDs, which impedes their commercialization. With an increase in the device EQE, stability is the major drawback that must be solved. Strategies to enhance stability will be aided by researching the following aspects: intrinsic instability of perovskite materials and degradation mechanism of PeLEDs, which require meticulous and systematic exploration.

**Efficient blue PeLEDs with a synergetic EL stability enhancement deserve more efforts.** The relatively poor performance of blue PeLEDs originates from unsatisfactory EQE and inferior operation stability. Blue emitters can be achieved by mixed halide perovskites, which always undergo EL redshift stemming from phase segregation. Blue PeLEDs from reduced-dimensional perovskites suffer from the inefficiency of electrically-driven carrier injection and difficulty of single-phase control. Exploring ways to produce efficient and stable blue PeLEDs is an essential and challenging subject that must be addressed in the future.

**Efficiency-oriented exploration of new materials and process methods requires further studies.** As discussed above, solution-processed Pb-based PeLEDs have been considerably improved in the past few years; however, the high toxicity of lead and relatively low reproducibility cast doubt on their potential commercialization. Electroluminescent devices that are based on lead-free perovskites or perovskite derivatives are one direction that is worth further exploration. The other worthwhile direction is to identify more commercially viable fabrication strategies.

**Table 1** Performance list of PeLEDs with record EQEs for different emission bands

| color | perovskites | dimensionality | EL /nm | device structure | EQE /% | $L_{max}$ /(cd·m$^{-2}$) | current efficiency /(cd·A$^{-1}$) | stability | area /cm$^2$ | FWHM /nm | CIE | note | publication date |
|---|---|---|---|---|---|---|---|---|---|---|---|---|---|
| blue | $CsPbBr_3$:PEACl:2%$YCl_3$ [6] ($CsPbBr_3$:PEACl:10% $YCl_3$) | quasi-2D | 485 (477) | glass/ITO/PEDOT:PSS/perovskite/TPBi/LiF/Al | **11.8** (4.8) | **9040** (~6000) | NA | $L_0$ = 100 cd/m$^2$@3.2 V, $T_{50}$~100 min spectral stability: 120 min@3.2 V; negligible spectrum variation under varied biases | 0.1 | NA | (0.09, 0.19) ((0.10, 0.13)) | stable bright | Dec. 2019 |
| | $PBABr_{1.1}(Cs_{0.7}FA_{0.3}PbBr_3)$ [7] | quasi-2D | 483 | glass/ ITO/$NiO_x$/TFB/PVK/perovskite/TPBi/LiF/Al | 9.5 | ~700 | ~12 | $L_0$ = 100 cd/m$^2$@1 mA/cm$^2$, $T_{50}$~250 s spectral stability: ~1600 s@ 0.2 mA/cm$^2$; shape of the EL spectrum does not change at increasing bias up to 6 V | 0.0324 | 26 | (0.094, 0.184) | | Aug. 2019 |
| | $CsPbCl_{0.9}Br_{2.1}$ + 100% PEABr [11] | quasi-2D | 480 | glass/ITO/PEDOT:PSS/perovskite/TPBi/LiF/Al | 5.7 | 3780 | 6.1 | $T_{50}$ (EQE drops to 50% of its initial value) = 10 min@4.4 V spectral stability: 1 min@4.4 V; increasing voltage, the spectrum is stable from 3.6 to 5.6 V, exceeding 6 V, spectrum red shifted slightly by around 8 nm | 0.1 | 21 | (0.102, 0.178) | | Mar. 2019 |
| | $BA_2Cs_{n-1}Pb_n(Br/Y)_{3n+1}$ [12] | quasi-2D | 465 (487) | glass/ITO/PEDOT:PSS/PVK/perovskite/TPBi/Al | 2.4 (6.2) | 962 (3340) | NA | $T_{70}$ (EQE drops to 70% of its initial value) ~10 min spectral stability: 5 min@6 V (78 mA/cm$^2$) (15 min@7 V, 35 mA/cm$^2$) | NA | 23 (22) | NA | | Jan. 2019 |
| | $PEA_2Cs_{1.6}MA_{0.4}Pb_3Br_{10}$ DPPOCl [13] | quasi-2D | 479 (489) | glass/ITO/PEDOT:PSS/PFI/perovskite/TPBi/LiF/Al | 5.2 (1.3) | 468 (5141) | NA | $L_0$ = 100 cd/m$^2$, $\boldsymbol{T_{50}}$ **= 90 min** spectral stability: wavelength shift is zero between half and maximum luminance ($L_0$ = 1500 cd/m$^2$, $T_{50}$ = 51 min@50 mA/cm$^2$) | 0.0614 | 18 | NA | stable | Mar. 2020 |
| | (Cs/Rb/FA/PEA/K)Pb $(Cl/Br)_3$ [14] | quasi-2D | 484 | glass/ITO/LiF/perovskite/LiF/Bphen/LiF/Al | 2.01 | 4015 | 2.11 | $L_0$ = 80 cd/m$^2$, $\boldsymbol{T_{50}}$ **= 300 min**@25 mA/cm$^2$ EL wavelength undergoes a red shift of about 8 nm after continuous operation at 25 mA/cm$^2$ for a period of time | 0.12 | ~24 | (0.135, 0.198) | stable | Feb. 2020 |
| | $PEA_2(Rb_{0.6}Cs_{0.4})_2Pb_3Br_{10}$ [15] $PEA_2(Rb_{0.4}Cs_{0.6})_2Pb_3Br_{10}$ | quasi-2D | 475 (490) | glass/ITO/PEDOT:PSS/perovskite/TmPyPB/LiF/Al | 1.35 (1.48) | 100.6 | NA | $L_0$ = 15 cd/m$^2$@4.5 V, $\boldsymbol{T_{50}}$ **= 14.5 min**; spectral stability: EL spectra changes negligibly under continuous operation for 20 min. ($\boldsymbol{T_{50}}$ **= 18.7 min**@4 V) | NA | 20 | (0.115, 0.099) | stable | Aug. 2019 |
| | Ca-TPBO-$CsPbBr_xCl_{3-x}$ [16] | QD | **463** | glass/ITO/PEDOT:PSS/TFB/PFI/perovskite/TPBi/LiF/Al | **3.3** | 569 | NA | NA | NA | 17 | NA | | Mar. 2020 |
| | P-$PDABr_2$-Cs $PbBr_3$ [17] | quasi-2D | 465 | ITO/PVK/PFI/perovskite/TPYMB/Liq/Al | 2.6 | 211 | NA | $T_{50}$ = 13.5 min@peak EQE (0.35 mA/cm$^2$) | NA | 25 | (0.145, 0.05) | | Sep. 2019 |

(*Continued*)

| color | perovskites | dimen-sionality | EL /nm | device structure | EQE /% | $L_{max}$ /(cd·m$^{-2}$) | current efficiency /(cd·A$^{-1}$) | stability | area /cm$^2$ | FWHM /nm | CIE | note | publication date |
|---|---|---|---|---|---|---|---|---|---|---|---|---|---|
| green | quasi-core/shell $CsPbBr_3$/MABr (mixture 1.0) [3] | 3D | 525 | glass/ITO/PEDOT:PSS/perovskite/PMMA/B3PYMPM/LiF/Al | 20.3 | 14000 | 78 | $L_0$ = 7130 cd/m$^2$, $T_{50}$~10.42 min@167 mA/cm$^2$; estimating $T_{50}$ at 100 cd/m$^2$ to be about 100 h | 0.03 | 20 | (0.18, 0.75) | | Oct. 2018 |
| | $CsPbBr_3$ + PEABr + PEG [19] | quasi-2D | 514 | glass/ITO/ZnO/PEDOT:PSS/perovskite/TPBi/LiF/Al | **28.2** | ~$10^4$ | 88.7 | NA | 0.1 | 18 | (0.088, 0.764) | out-coupling | Apr. 2019 |
| | $CsPbBr_3$ + PEABr + PEG [19] | quasi-2D | 512 | PET/Ag NWs/pattern ZnO/ETA-PEDOT/perovskite/TPBi/LiF/Al | 24.5 (17) | ~$10^4$ | 75 | $L_0$ = 100 cd/m$^2$, $T_{50}$~7.56 h | 0.1 | NA | (0.079, 0.751) | out-coupling flexible | Mar. 2020 |
| | $MAPbBr_3$:TPBi [20] | 3D | 540 | glass/self-organized conducting polymer (SOCP) anode/perovskite/TPBi/LiF/Al | 21.8 | NA | 87.35 | $L_0$ = 100 cd/m$^2$, $T_{50}$ = 250 min | NA | NA | NA | out-coupling | Apr. 2019 |
| | TFA-derived $CsPbBr_3$ [21] ($FA_{0.11}MA_{0.10}Cs_{0.79}PbBr_3$) | 3D | 518 | glass/ITO/PEDOT:PSS/perovskite/TPBi/LiF/Al | 10.5 (17) | 16436 (35700) | 32 | $L_0$ = 100 cd/m$^2$, **$T_{50}$ = 250 h** | NA | NA | NA | stable | Feb. 2019 |
| | $CsPbBr_3$-PEO-CF [22] | 3D | 525 | glass/ITO/PEDOT:PSS/perovskite/TPBi/LiF/Al | 4.76 | 51890 | NA | under ambient conditions (relative humidity ~60%), **$L_0$ ≈ 1000 cd/m$^2$, $T_{82}$ = 80 h** | 0.0725 | 20 | NA | stable | May. 2017 |
| | KBr-$CsPbBr_3$ [23] | 3D | ~520 | glass/ITO/ Poly-TPD/PVK/perovskite in $SiO_2$ aperture (100 nm)/TPBi/LiF/Al | 7.7 | **7646206** | NA | NA | NA | NA | NA | bright | Apr. 2020 |
| | $CsPbBr_3$ [24] | 3D | 523 | glass/ITO/a-ZSO/perovskite/NPD/MoOx/Ag | 9.3 | **496320** | 37 | NA | NA | 16 | NA | bright | Jul. 2019 |
| red | $CsPb(Br/I)_3$ [5] | QD | 653 | glass/ITO/PEDOT:PSS/poly-TPD/perovskite/TPBi/Liq/Al | 21.3 | 500 (794) | 10.6 | $L_0$ = 100 cd/m$^2$,$T_{50}$ = 5 min@1.25 mA/cm$^2$ (for An-HI-based LED, $T_{50}$ = 180 min) | 0.02 | 33 | (0.72, 0.28) | | Oct. 2018 |
| | FPMATFA-$FA_{0.33}Cs_{0.67}Pb(I_{0.7}Br_{0.3})_3$ [25] | 3D | 694 | glass/ITO/poly-TPD/perovskite/TPBi/LiF/Al | 20.9 | ~400 ($10^2$) | NA | in $N_2$ glove box, $L_0$ = 25 cd/m$^2$, **$T_{50}$ = 14 h**@2.5 mA/cm$^2$ | 0.04 | 37 | (0.732, 0.268) | stable | Feb. 2020 |
| | PEDXA-$CsPbBr_{0.6}I_{2.4}$ [26] | 3D | 668 | glass/ITO/ZnMgO/perovskite/poly-TPD/$MoO_3$/Ag | 6.55 | 338 | 1.36 | **$L_0$ = 300 cd/m$^2$, $T_{50}$ = 0.5 h.** no change in EL spectra was observed at different applied voltages | NA | 32 | (0.726, 0.274) | stable | Nov. 2018 |
| | Zr-$CsPbI_3$ [27] | QD | 686 | Si/Ag/ZnO/PEI/perovskite/TCTA/$MoO_3$/Au | 13.7 | 14725 | NA | efficiency drop ~8.7% under 500 mA/cm$^2$ | NA | NA | (0.71, 0.28) | stable | Mar. 2020 |

(*Continued*)

| color | perovskites | dimen-sionality | EL /nm | device structure | EQE /% | $L_{max}$ /(cd·m$^{-2}$) | current efficiency /(cd·A$^{-1}$) | stability | area /cm$^2$ | FWHM /nm | CIE | note | publication date |
|---|---|---|---|---|---|---|---|---|---|---|---|---|---|
| | 4-F-PMAI-$CsPbI_3$ ($CsPbI_{2.8}Br_{0.2}$) [28] | QD | 692 (689) | ITO/poly-TPD/per-ovskite/TPBi/LiF/Al | 14.8 (18.6) | NA | NA | $L_0$ = 100 cd/m$^2$, $T_{50}$ ~20 h@5 mA/cm$^2$ | 0.04 | 36 | (0.72, 0.27) | stable | Mar. 2020 |
| | $CsPbBrI_2$ [24] | 3D | 650 | glass/ITO/a-ZSO/ perovskite/NPD/ $MoO_x$/Ag | 4.6 | 20000 | 2.5 | NA | NA | 40 | NA | bright | Jul. 2019 |
| near-infrared | ODEA-$FAPbI_3$ [29] | 3D | 800 | glass/ITO/ZnO: PEIE/perovskite/ TPB/$MoO_x$/Au | 21.6 | NA | NA | in the glovebox without encapsulation, $T_{50}$ (EQE drops to its 50%) = 20 h@25 mA/cm$^2$ | 0.0725 | NA | NA | | Mar. 2019 |
| | 5AVA-$FAPbI_3$ [2] | 3D | 803 | glass/ITO/PEIE-ZnO/perovskite/ TPB/$MoO_3$/Au | 20.7 | NA | NA | with glass-epoxy encapsulation, $T_{50}$ = 20 h@100 mA/cm$^2$ | 0.03 | 75 meV | NA | | Oct. 2018 |
| | perovskite-polymer ($(NMA)_2(FA)Pb_2I_7$-poly-HEMA) [30] | quasi-2D | ~795 | glass/ITO/MZO/ PEIE/perovskite/ TPB-PFO/$MoO_x$/Au | 20.1 | NA | NA | encapsulated with epoxy adhesive/cover glass in air, the EL half-life $T_{50}$ = 46 h@peak EQE (0.1 mA/cm$^2$) | NA | ~49 | NA | | Nov. 2018 |
| | 5-AVA-$FAPbI_3$ [31] | 3D | 799 | glass/ITO/ZnO/ PEIE/perovskite/ poly-TPD/$MoO_3$/Al | 20.2 (12.1) | NA | NA | $T_{80}$ = 20 h@peak EQE (57 mA/cm$^2$) (large-area $T_{50}$ = 10 h@10 mA/cm$^2$ | 0.04 | 41 | NA | large-area (9 cm$^2$) | Apr. 2020 |
| | $(PEA)_2PbI_4$-$FA_{0.98}Cs_{0.02}PbI_3$ [32] | 2D/3D | ~810 | glass/ITO/ZnO nano-particle/perovskite/ poly-TPD/$MoO_3$/Ag | NA | NA | NA | $L_0 \approx$ 10 W/(sr·m$^2$), after 100 h, it is ≈ 135% of initial radiance, estimating **$T_{50}$>200 h** | NA | NA | NA | stable | Feb. 2020 |

Notes: NA—not available. $L_0$—initial luminance. $T_{50/80}$—time when $L_0$ (or EQE) decreases to 50% or 80% of its initial value

**Table 2** Performance list of vacuum deposited PeLEDs

| color | perovskite | dimensionality | method | device structure | EL /nm | $L_{max}$ /(cd·m$^{-2}$) | current efficiency /(cd·A$^{-1}$) | EQE /% | publication date |
|---|---|---|---|---|---|---|---|---|---|
| blue | Cs-Pb-Br-Cl [33] | 3D | co-evaporation | ITO/$NiO_x$/perovskite/TPBi/LiF/Al | 468 | 121 | 0.21 | **0.38** | Nov. 2019 |
| green | $MAPbBr_3$ [34] | 3D | vacuum evaporated $PbBr_2$ + CVD MABr | ITO + PFN-OX/perovskite/$MoO_3$/Au | 532 | 560 | NA | 0.016 | Jun. 2017 |
| | $CsPbBr_3$ [35] | 3D | co-evaporation | ITO/PEDOT/poly-TPD/perovskite/TmPyPB/Liq/Al | 520 | 57.65 | 5.75 | 1.55 | Jul. 2017 |
| | PEA-$MAPbBr_3$ [36] | quasi-2D | layer-by-layer deposition | ITO/PEDOT/perovskite/TPBi/Liq/Al | 531 | 6200 | 1.3 | 0.36 | Oct. 2017 |
| | $CsPbBr_3$ [37] | 3D | vacuum evaporated $PbBr_2$ + dipping CsBr | ITO/ZnO/perovskite/$NiO_x$/Au | 522 | NA | NA | NA | Apr. 2018 |
| | $CsPbBr_3$ [38] | 3D | CVD | Au/MgO/perovskite/n-MgZnO/$n^+$-GaN | 538 | 5025 | 1.92 | 1.46 | Sep. 2018 |
| | $CsPbBr_3$ [39] | 3D | co-evaporation | ITO/PEDOT/perovskite/TPBi/LiF/Al | 519 | 53486 | NA | 2.5 | Feb. 2019 |
| | $CsPbBr_3$ [40] | 3D | layer-by-layer deposition | ITO/PVK/perovskite/TPBi/LiF/Al | 525 | 904 | NA | 0.3 | Mar. 2019 |
| | $CsPbBr_3$ [10] | 3D | co-evaporation | ITO/$NiO_x$/perovskite/TPBi/LiF/Al | 516 | 9442 | 10.15 | 3.26 | Oct. 2019 |
| | $CsPbBr_3$ [41] | 3D | co-evaporation | ITO/PEDOT:PSS/perovskite/TmPyP8/Lq/Al | 524 | 1607 | 1.07 | NA | Jan. 2020 |
| | PEA-$CsPbBr_3$ [42] | 3D | layer-by-layer deposited $CsPbBr_3$ + spin-coated PEABr | ITO/PEDOT:PSS/perovskite/TPBi/LiF/Al | 529 | 5684 | 14.64 | **4.1** | Mar. 2020 |
| red | $CsSnBr_3$ [43] | 3D | layer-by-layer deposition | ITO/LiF/perovskite/LiF/ZnS/Ag | 672 | 172 | 0.65 | 0.34 | Mar. 2018 |
| near-infrared | $MAPb(I/Br)_3$ [44] | 3D | dual-source evaporated $MAPbI_3$ + evaporated $PbBr_2$ + spin-coated MABr | ITO/PEDOT/poly-TPD/perovskite/PCBM/Ba/Ag | **784** | ~300 | NA | 0.06 | Sep. 2015 |
| | $MAPbI_3$ [45] | 3D | co-evaporation | ITO/$C_{60}$/perovskite/TaTm/Au | 760 | NA | NA | **1.92** | Sep. 2018 |

**Table 3** Performance list of lead-free LEDs

| color | method | perovskite | EL /nm | device structure | EQE /% | current efficiency /(cd·A$^{-1}$) | $L_{max}$ /(cd·m$^{-2}$) | FWHM/nm | publication date |
|---|---|---|---|---|---|---|---|---|---|
| near-infrared | spin-coating | $CH_3NH_3Sn(Br_{1-x}I_x)_3$ [51] | 945 | ITO/PEDOT:PSS/perovskite /F8/Ca/Ag | 0.72 | NA | NA | 130 meV | Jun. 2016 |
| near-infrared | spin-coating | $CsSnI_3$ [52] | 950 | ITO/PEDOT/perovskite/PBD/LiF/Al | 3.8 | NA | NA | > 100 | Jul. 2016 |
| red | spin-coating | $PEA_2SnI_4$ [53] | 618 | ITO/PEDOT:PSS/perovskite/F8/LiF/Al | NA | 0.029 | 0.15 | ~50 | Jun. 2017 |
| red | layer-by-layer deposition | $CsSnBr_3$ [43] | 672 | ITO/LiF/$CsSnBr_3$/LiF/ZnS/Ag | 0.34 | 0.65 | 172 | ~54 | Mar. 2018 |
| blue | spin-coating | $Cs_3Cu_2I_5$ [54] | 440 | ITO/ZSO/$Cs_3Cu_2I_5$/NPD/$MoO_x$/Ag | NA | NA | 10 | > 70 | Sep. 2018 |
| white | layer-by-layer deposition | $Cs_2Ag_{0.6}Na_{0.4}InCl_6$ [55] | 560 | glass/PEIE-ITO/PEIE-ZnO/perovskite/TAPC/$MoO_3$/Al | NA | 0.11 | ~50 | ~170 | Nov. 2018 |
| orange | spin-coating | $(C_{18}H_{35}NH_3)_2SnBr_4$ [56] | 621 | ITO/ZnO/PEI/perovskite/TCTA/$MoO_3$/Al | 0.1 | NA | 350 | ~163 | Jan. 2019 |
| near-infrared | vapor-anion-exchange | $Cs_3Sb_2I_9$ [57] | > 750 | ITO/PEDOT/perovskite/TPBi/LiF/Al | NA | NA | NA | > 120 | Aug. 2019 |
| violet | spin-coating | $Cs_3Sb_2Br_9$ [58] | 408 | ITO/ZnO/PEI/perovskite/TCTA/$MoO_3$/Al | 0.206 | NA | 29.6 | ~70 | Feb. 2020 |
| red | spin-coating | $PEA_2SnI_4$ [59] | 633 | ITO/PEDOT:PSS/perovskite/TPBi/LiF/Al | 0.3 | NA | 70 | 24 | Mar. 2020 |
| yellow | spin-coating | $CsCu_2I_3$ [60] | 550 | ITO/PEDOT:PSS/poly-TPD/perovskite/TPBi/LiF/Al | 0.17 | NA | 47.5 | ~100 | Mar. 2020 |
| blue | spin-coating | $Cs_3Cu_2I_5$ [61] | 445 | ITO/P-NiO/perovskite/TPBi/LiF/Al | 1.12 | NA | 263.2 | ~63 | Apr. 2020 |

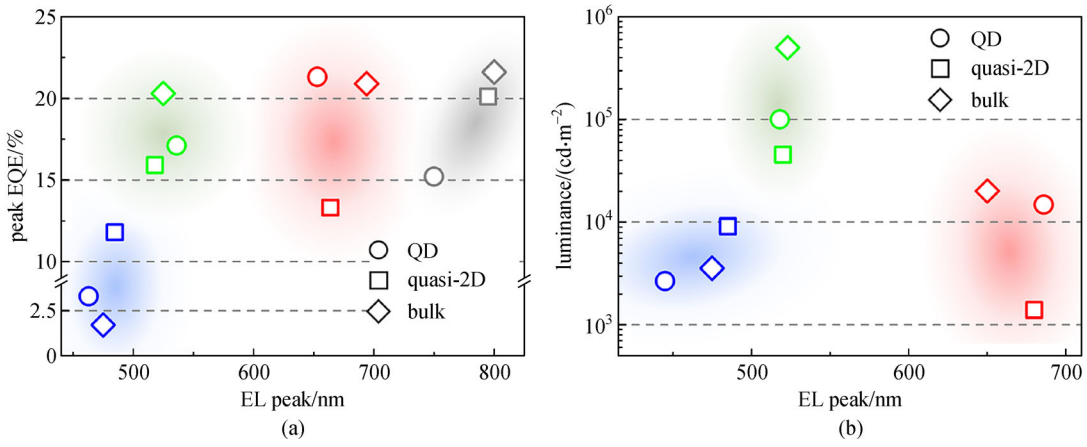


**Fig. 1** (a) Best EQEs [3,5,6,16,25,29,30,63–67] and (b) highest luminance [6,24,27,63,68–71] of bulk, quasi-2D, and quantum dot PeLEDs

Inkjet printing or electrohydrodynamic printing is the top choice for the fabrication of ultra-large-size displays. Thermal evaporation (preferably single-sourced), which is compatible with existing OLED manufacturing lines, also deserves more research attention. More efforts must be devoted to these new technologies to improve their performance through composition, morphology, grain engineering, and device physics.

**Acknowledgements** This work was supported by the National Key R&D Program of China (No. 2016YFB070700702), the National Natural Science Foundation of China (Grant No. 51761145048), the Fundamental Research Funds for the Central Universities (HUST:2019421JYCXJJ004) and the Innovation Funds of Wuhan National Laboratory for Optoelectronics (WNLO).

## References

1. Lee T W. Emerging halide perovskite materials and devices for optoelectronics. Advanced Materials, 2019, 31(47): e1905077
2. Cao Y, Wang N, Tian H, Guo J, Wei Y, Chen H, Miao Y, Zou W, Pan K, He Y, Cao H, Ke Y, Xu M, Wang Y, Yang M, Du K, Fu Z, Kong D, Dai D, Jin Y, Li G, Li H, Peng Q, Wang J, Huang W. Perovskite light-emitting diodes based on spontaneously formed submicrometre-scale structures. Nature, 2018, 562(7726): 249–253
3. Lin K, Xing J, Quan L N, de Arquer F P G, Gong X, Lu J, Xie L, Zhao W, Zhang D, Yan C, Li W, Liu X, Lu Y, Kirman J, Sargent E H, Xiong Q, Wei Z. Perovskite light-emitting diodes with external quantum efficiency exceeding 20 percent. Nature, 2018, 562(7726): 245–248
4. Tan Z K, Moghaddam R S, Lai M L, Docampo P, Higler R, Deschler F, Price M, Sadhanala A, Pazos L M, Credgington D, Hanusch F, Bein T, Snaith H J, Friend R H. Bright light-emitting diodes based on organometal halide perovskite. Nature Nanotechnology, 2014, 9 (9): 687–692
5. Chiba T, Hayashi Y, Ebe H, Hoshi K, Sato J, Sato S, Pu Y J, Ohisa S, Kido J. Anion-exchange red perovskite quantum dots with ammonium iodine salts for highly efficient light-emitting devices. Nature Photonics, 2018, 12(11): 681–687
6. Wang Q, Wang X, Yang Z, Zhou N, Deng Y, Zhao J, Xiao X, Rudd P, Moran A, Yan Y, Huang J. Efficient sky-blue perovskite light-emitting diodes via photoluminescence enhancement. Nature Communications, 2019, 10(1): 5633
7. Liu Y, Cui J, Du K, Tian H, He Z, Zhou Q, Yang Z, Deng Y, Chen D, Zuo X, Ren Y, Wang L, Zhu H, Zhao B, Di D, Wang J, Friend R H, Jin Y. Efficient blue light-emitting diodes based on quantum-confined bromide perovskite nanostructures. Nature Photonics, 2019, 13(11): 760–764
8. Meredith P, Armin A. LED technology breaks performance barrier. Nature, 2018, 562(7726): 197–198
9. Anaya M, Rand B P, Holmes R J, Credgington D, Bolink H J, Friend R H, Wang J, Greenham N C, Stranks S D. Best practices for measuring emerging light-emitting diode technologies. Nature Photonics, 2019, 13(12): 818–821
10. Li J, Du P, Li S, Liu J, Zhu M, Tan Z, Hu M, Luo J, Guo D, Ma L, Nie Z, Ma Y, Gao L, Niu G, Tang J. High-throughput combinatorial optimizations of perovskite light-emitting diodes based on all-vacuum deposition. Advanced Functional Materials, 2019, 29(51): 1903607
11. Li Z, Chen Z, Yang Y, Xue Q, Yip H L, Cao Y. Modulation of recombination zone position for quasi-two-dimensional blue perovskite light-emitting diodes with efficiency exceeding 5. Nature Communications, 2019, 10(1): 1027
12. Vashishtha P, Ng M, Shivarudraiah S B, Halpert J E. High efficiency blue and green light-emitting diodes using ruddlesden–popper inorganic mixed halide perovskites with butylammonium interlayers. Chemistry of Materials, 2019, 31(1): 83–89
13. Ma D, Todorović P, Meshkat S, Saidaminov M I, Wang Y K, Chen B, Li P, Scheffel B, Quintero-Bermudez R, Fan J Z, Dong Y, Sun B, Xu C, Zhou C, Hou Y, Li X, Kang Y, Voznyy O, Lu Z H, Ban D, Sargent E H. Chloride insertion–immobilization enables bright, narrowband, and stable blue-emitting perovskite diodes. Journal of the American Chemical Society, 2020, 142(11): 5126–5134
14. Yuan F, Ran C, Zhang L, Dong H, Jiao B, Hou X, Li J, Wu Z. A

cocktail of multiple cations in inorganic halide perovskite toward efficient and highly stable blue light-emitting diodes. ACS Energy Letters, 2020, 5(4): 1062–1069

15. Jiang Y, Qin C, Cui M, He T, Liu K, Huang Y, Luo M, Zhang L, Xu H, Li S, Wei J, Liu Z, Wang H, Kim G H, Yuan M, Chen J. Spectra stable blue perovskite light-emitting diodes. Nature Communications, 2019, 10(1): 1868
16. Yao J, Wang L, Wang K, Yin Y, Yang J, Zhang Q, Yao H. Calcium-tributylphosphine oxide passivation enables the efficiency of pure-blue perovskite light-emitting diode up to 3.3%. Science Bulletin, 2020, doi:10.1016/j.scib.2020.03.036
17. Yuan S, Wang Z K, Xiao L X, Zhang C F, Yang S Y, Chen B B, Ge H T, Tian Q S, Jin Y, Liao L S. Optimization of low-dimensional components of quasi-2D perovskite films for deep-blue light-emitting diodes. Advanced Materials, 2019, 31(44): e1904319
18. Shen Y, Cheng L P, Li Y Q, Li W, Chen J D, Lee S T, Tang J X. High-efficiency perovskite light-emitting diodes with synergetic outcoupling enhancement. Advanced Materials, 2019, 31(24): e1901517
19. Shen Y, Li M N, Li Y, Xie F M, Wu H Y, Zhang G H, Chen L, Lee S T, Tang J X. Rational interface engineering for efficient flexible perovskite light-emitting diodes. ACS Nano, 2020, acsnano.0c01908
20. Park M H, Park J, Lee J, So H S, Kim H, Jeong S H, Han T H, Wolf C, Lee H, Yoo S, Lee T W. Efficient perovskite light-emitting diodes using polycrystalline core–shell-mimicked nanograins. Advanced Functional Materials, 2019, 29(22): 1902017
21. Wang H, Zhang X, Wu Q, Cao F, Yang D, Shang Y, Ning Z, Zhang W, Zheng W, Yan Y, Kershaw S V, Zhang L, Rogach A L, Yang X. Trifluoroacetate induced small-grained $CsPbBr_3$ perovskite films result in efficient and stable light-emitting devices. Nature Communications, 2019, 10(1): 665
22. Wu C, Zou Y, Wu T, Ban M, Pecunia V, Han Y, Liu Q, Song T, Duhm S, Sun B. Improved performance and stability of all-inorganic perovskite light-emitting diodes by antisolvent vapor treatment. Advanced Functional Materials, 2017, 27(28): 1700338
23. Zou C, Liu Y, Ginger D S, Lin L Y. Suppressing efficiency roll-off at high current densities for ultra-bright green perovskite light-emitting diodes. ACS Nano, 2020, acsnano.0c01817
24. Sim K, Jun T, Bang J, Kamioka H, Kim J, Hiramatsu H, Hosono H. Performance boosting strategy for perovskite light-emitting diodes. Applied Physics Reviews, 2019, 6(3): 031402
25. Fang Z, Chen W, Shi Y, Zhao J, Chu S, Zhang J, Xiao Z. Dual passivation of perovskite defects for light-emitting diodes with external quantum efficiency exceeding 20%. Advanced Functional Materials, 2020, 30(12): 1909754
26. Cai W, Chen Z, Li Z, Yan L, Zhang D, Liu L, Xu Q H, Ma Y, Huang F, Yip H L, Cao Y. Polymer-assisted *in situ* growth of all-inorganic perovskite nanocrystal film for efficient and stable pure-red light-emitting devices. ACS Applied Materials & Interfaces, 2018, 10 (49): 42564–42572
27. Lu M, Guo J, Sun S, Lu P, Wu J, Wang Y, Kershaw S V, Yu W W, Rogach A L, Zhang Y. Bright $CsPbI_3$ perovskite quantum dot light-emitting diodes with top-emitting structure and a low efficiency roll-off realized by applying zirconium acetylacetonate surface modification. Nano Letters, 2020, 20(4): 2829–2836
28. Cheng G, Liu Y, Chen T, Chen W, Fang Z, Zhang J, Ding L, Li X, Shi T, Xiao Z. Efficient all-inorganic perovskite light-emitting diodes with improved operation stability. ACS Applied Materials & Interfaces, 2020, 12(15): 18084–18090
29. Xu W, Hu Q, Bai S, Bao C, Miao Y, Yuan Z, Borzda T, Barker A J, Tyukalova E, Hu Z, Kawecki M, Wang H, Yan Z, Liu X, Shi X, Uvdal K, Fahlman M, Zhang W, Duchamp M, Liu J M, Petrozza A, Wang J, Liu L M, Huang W, Gao F. Rational molecular passivation for high-performance perovskite light-emitting diodes. Nature Photonics, 2019, 13(6): 418–424
30. Zhao B, Bai S, Kim V, Lamboll R, Shivanna R, Auras F, Richter J M, Yang L, Dai L, Alsari M, She X J, Liang L, Zhang J, Lilliu S, Gao P, Snaith H J, Wang J, Greenham N C, Friend R H, Di D. High-efficiency perovskite–polymer bulk heterostructure light-emitting diodes. Nature Photonics, 2018, 12(12): 783–789
31. Zhao X, Tan Z K. Large-area near-infrared perovskite light-emitting diodes. Nature Photonics, 2020, 14(4): 215–218
32. Han T H, Lee J W, Choi Y J, Choi C, Tan S, Lee S J, Zhao Y, Huang Y, Kim D, Yang Y. Surface-2D/bulk-3D heterophased perovskite nanograins for long-term-stable light-emitting diodes. Advanced Materials, 2020, 32(1): e1905674
33. Du P, Li J, Wang L, Liu J, Li S, Liu N, Li Y, Zhang M, Gao L, Ma Y, Tang J. Vacuum-deposited blue inorganic perovskite light-emitting diodes. ACS Applied Materials & Interfaces, 2019, 11(50): 47083–47090
34. Leyden M R, Meng L, Jiang Y, Ono L K, Qiu L, Juarez-Perez E J, Qin C, Adachi C, Qi Y. Methylammonium lead bromide perovskite light-emitting diodes by chemical vapor deposition. Journal of Physical Chemistry Letters, 2017, 8(14): 3193–3198
35. Hu Y, Wang Q, Shi Y L, Li M, Zhang L, Wang Z K, Liao L S. Vacuum-evaporated all-inorganic cesium lead bromine perovskites for high-performance light-emitting diodes. Journal of Materials Chemistry C, Materials for Optical and Electronic Devices, 2017, 5 (32): 8144–8149
36. Chiang K M, Hsu B W, Chang Y A, Yang L, Tsai W L, Lin H W. Vacuum-deposited organometallic halide perovskite light-emitting devices. ACS Applied Materials & Interfaces, 2017, 9(46): 40516–40522
37. Zhuang S, Ma X, Hu D, Dong X, Zhang B. Air-stable all inorganic green perovskite light emitting diodes based on $ZnO/CsPbBr_3/NiO$ heterojunction structure. Ceramics International, 2018, 44(5): 4685–4688
38. Shi Z, Lei L, Li Y, Zhang F, Ma Z, Li X, Wu D, Xu T, Tian Y, Zhang B, Yao Z, Du G. Hole-injection layer-free perovskite light-emitting diodes. ACS Applied Materials & Interfaces, 2018, 10(38): 32289–32297
39. Lian X, Wang X, Ling Y, Lochner E, Tan L, Zhou Y, Ma B, Hanson K, Gao H. Light emitting diodes based on inorganic composite halide perovskites. Advanced Functional Materials, 2019, 29(5): 1807345
40. Tan Y, Li R, Xu H, Qin Y, Song T, Sun B. Ultrastable and reversible fluorescent perovskite films used for flexible instantaneous display. Advanced Functional Materials, 2019, 29(23): 1900730
41. Shin M, Lee H S, Sim Y C, Cho Y H, Cheol Choi K, Shin B. Modulation of growth kinetics of vacuum-deposited $CsPbBr_3$ films for efficient light-emitting diodes. ACS Applied Materials &

Interfaces, 2020, 12(1): 1944–1952
42. Jia K, Song L, Hu Y, Guo X, Liu X, Geng C, Xu S, Fan R, Huang L, Luan N, Bi W. Improved performance for thermally evaporated perovskite light-emitting devices via defect passivation and carrier regulation. ACS Applied Materials & Interfaces, 2020, 12(13): 15928–15933
43. Yuan F, Xi J, Dong H, Xi K, Zhang W, Ran C, Jiao B, Hou X, Jen A K Y, Wu Z. All-inorganic hetero-structured cesium tin halide perovskite light-emitting diodes with current density over 900 $A \cdot cm^{-2}$ and its amplified spontaneous emission behaviors. Physica Status Solidi (RRL)–Rapid Research Letters, 2018, 12(5): 1800090
44. Gil-Escrig L, Miquel-Sempere A, Sessolo M, Bolink H J. Mixed iodide–bromide methylammonium lead perovskite-based diodes for light emission and photovoltaics. Journal of Physical Chemistry Letters, 2015, 6(18): 3743–3748
45. Dänekamp B, Droseros N, Palazon F, Sessolo M, Banerji N, Bolink H J. Efficient photo- and electroluminescence by trap states passivation in vacuum-deposited hybrid perovskite thin films. ACS Applied Materials & Interfaces, 2018, 10(42): 36187–36193
46. Leng M, Yang Y, Chen Z, Gao W, Zhang J, Niu G, Li D, Song H, Zhang J, Jin S, Tang J. Surface passivation of bismuth-based perovskite variant quantum dots to achieve efficient blue emission. Nano Letters, 2018, 18(9): 6076–6083
47. Leng M, Yang Y, Zeng K, Chen Z, Tan Z, Li S, Li J, Xu B, Li D, Hautzinger M P, Fu Y, Zhai T, Xu L, Niu G, Jin S, Tang J. All-inorganic bismuth-based perovskite quantum dots with bright blue photoluminescence and excellent stability. Advanced Functional Materials, 2018, 28(1): 1704446
48. Tan Z, Li J, Zhang C, Li Z, Hu Q, Xiao Z, Kamiya T, Hosono H, Niu G, Lifshitz E, Cheng Y, Tang J. Highly efficient blue-emitting Bi-doped $Cs_2SnCl_6$ perovskite variant: photoluminescence induced by impurity doping. Advanced Functional Materials, 2018, 28(29): 1801131
49. Hu Q, Deng Z, Hu M, Zhao A, Zhang Y, Tan Z, Niu G, Wu H, Tang J. X-ray scintillation in lead-free double perovskite crystals. Science China, Chemistry, 2018, 61(12): 1581–1586
50. Zhou C, Tian Y, Yuan Z, Lin H, Chen B, Clark R, Dilbeck T, Zhou Y, Hurley J, Neu J, Besara T, Siegrist T, Djurovich P, Ma B. Highly efficient broadband yellow phosphor based on zero-dimensional tin mixed-halide perovskite. ACS Applied Materials & Interfaces, 2017, 9(51): 44579–44583
51. Lai M L, Tay T Y S, Sadhanala A, Dutton S E, Li G, Friend R H, Tan Z K. Tunable near-infrared luminescence in tin-halide perovskite devices. Journal of Physical Chemistry Letters, 2016, 7(14): 2653–2658
52. Hong W L, Huang Y C, Chang C Y, Zhang Z C, Tsai H R, Chang N Y, Chao Y C. Efficient low-temperature solution-processed lead-free perovskite infrared light-emitting diodes. Advanced Materials, 2016, 28(36): 8029–8036
53. Lanzetta L, Marin-Beloqui J M, Sanchez-Molina I, Ding D, Haque S A. Two-dimensional organic tin halide perovskites with tunable visible emission and their use in light-emitting devices. ACS Energy Letters, 2017, 2(7): 1662–1668
54. Jun T, Sim K, Iimura S, Sasase M, Kamioka H, Kim J, Hosono H. Lead-free highly efficient blue-emitting $Cs_3Cu_2I_5$ with 0D electronic structure. Advanced Materials, 2018, 30(43): e1804547
55. Luo J, Wang X, Li S, Liu J, Guo Y, Niu G, Yao L, Fu Y, Gao L, Dong Q, Zhao C, Leng M, Ma F, Liang W, Wang L, Jin S, Han J, Zhang L, Etheridge J, Wang J, Yan Y, Sargent E H, Tang J. Efficient and stable emission of warm-white light from lead-free halide double perovskites. Nature, 2018, 563(7732): 541–545
56. Zhang X, Wang C, Zhang Y, Zhang X, Wang S, Lu M, Cui H, Kershaw S V, Yu W W, Rogach A L. Bright orange electroluminescence from lead-free two-dimensional perovskites. ACS Energy Letters, 2019, 4(1): 242–248
57. Singh A, Chiu N C, Boopathi K M, Lu Y J, Mohapatra A, Li G, Chen Y F, Guo T F, Chu C W. Lead-free antimony-based light-emitting diodes through the vapor–anion-exchange method. ACS Applied Materials & Interfaces, 2019, 11(38): 35088–35094
58. Ma Z, Shi Z, Yang D, Zhang F, Li S, Wang L, Wu D, Zhang Y, Na G, Zhang L, Li X, Zhang Y, Shan C. Electrically-driven violet light-emitting devices based on highly stable lead-free perovskite $Cs_3Sb_2Br_9$ quantum dots. ACS Energy Letters, 2020, 5(2): 385–394
59. Liang H, Yuan F, Johnston A, Gao C, Choubisa H, Gao Y, Wang Y K, Sagar L K, Sun B, Li P, Bappi G, Chen B, Li J, Wang Y, Dong Y, Ma D, Gao Y, Liu Y, Yuan M, Saidaminov M I, Hoogland S, Lu Z H, Sargent E H. High color purity lead-free perovskite light-emitting diodes via Sn stabilization. Advancement of Science, 2020, 7(8): 1903213
60. Ma Z, Shi Z, Qin C, Cui M, Yang D, Wang X, Wang L, Ji X, Chen X, Sun J, Wu D, Zhang Y, Li X J, Zhang L, Shan C. Stable yellow light-emitting devices based on ternary copper halides with broadband emissive self-trapped excitons. ACS Nano, 2020, 14 (4): 4475–4486
61. Wang L, Shi Z, Ma Z, Yang D, Zhang F, Ji X, Wang M, Chen X, Na G, Chen S, Wu D, Zhang Y, Li X, Zhang L, Shan C. Colloidal synthesis of ternary copper halide nanocrystals for high-efficiency deep-blue light-emitting diodes with a half-lifetime above 100 h. Nano Letters, 2020, 20(5): 3568–3576
62. Quan L N, Rand B P, Friend R H, Mhaisalkar S G, Lee T W, Sargent E H. Perovskites for next-generation optical sources. Chemical Reviews, 2019, 119(12): 7444–7477
63. Kim H P, Kim J, Kim B S, Kim H M, Kim J, Yusoff A, Jang J, Nazeeruddin M K. High-efficiency, blue, green, and near-infrared light-emitting diodes based on triple cation perovskite. Advanced Optical Materials, 2017, 5(7): 1600920
64. Wu C, Wu T, Yang Y, McLeod J A, Wang Y, Zou Y, Zhai T, Li J, Ban M, Song T, Gao X, Duhm S, Sirringhaus H, Sun B. Alternative type two-dimensional–three-dimensional lead halide perovskite with inorganic sodium ions as a spacer for high-performance light-emitting diodes. ACS Nano, 2019, 13(2): 1645–1654
65. Chen H, Fan L, Zhang R, Bao C, Zhao H, Xiang W, Liu W, Niu G, Guo R, Zhang L, Wang L. High-efficiency formamidinium lead bromide perovskite nanocrystal-based light-emitting diodes fabricated via a surface defect self-passivation strategy. Advanced Optical Materials, 2020, 8(6): 1901390
66. He Z, Liu Y, Yang Z, Li J, Cui J, Chen D, Fang Z, He H, Ye Z, Zhu H, Wang N, Wang J, Jin Y. High-efficiency red light-emitting diodes based on multiple quantum wells of phenylbutylammonium-cesium lead iodide perovskites. ACS Photonics, 2019, 6(3): 587–594
67. Xiao Z, Kerner R A, Tran N, Zhao L, Scholes G D, Rand B P.

Engineering perovskite nanocrystal surface termination for light-emitting diodes with external quantum efficiency exceeding 15%. Advanced Functional Materials, 2019, 29(11): 1807284

68. Deng W, Xu X, Zhang X, Zhang Y, Jin X, Wang L, Lee S T, Jie J. Organometal halide perovskite quantum dot light-emitting diodes. Advanced Functional Materials, 2016, 26(26): 4797–4802
69. Na Quan L, Ma D, Zhao Y, Voznyy O, Yuan H, Bladt E, Pan J, García de Arquer F P, Sabatini R, Piontkowski Z, Emwas A H, Todorović P, Quintero-Bermudez R, Walters G, Fan J Z, Liu M, Tan H, Saidaminov M I, Gao L, Li Y, Anjum D H, Wei N, Tang J, McCamant D W, Roeffaers M B J, Bals S, Hofkens J, Bakr O M, Lu Z H, Sargent E H. Edge stabilization in reduced-dimensional perovskites. Nature Communications, 2020, 11(1): 170
70. Song J, Fang T, Li J, Xu L, Zhang F, Han B, Shan Q, Zeng H. Organic–inorganic hybrid passivation enables perovskite QLEDs with an EQE of 16.48%. Advanced Materials, 2018, 30(50): e1805409
71. Tian Y, Zhou C, Worku M, Wang X, Ling Y, Gao H, Zhou Y, Miao Y, Guan J, Ma B. Highly efficient spectrally stable red perovskite light-emitting diodes. Advanced Materials, 2018, 30(20): e1707093

**Peipei Du** obtained the bachelor degree from Wuhan University of Science and Technology, China. She is currently pursuing a doctorate in the School of Materials Science and Engineering, Huazhong University of Science and Technology, China. Her research interests are mainly focused on the halide perovskite materials and their application in LEDs.

**Liang Gao** received his Ph.D. degree from Wuhan National Laboratory for Optoelectronics at Huazhong University of Science and Technology, China in 2018 and undertook his research under the supervision of Prof. Edward H. Sargent in University of Toronto, Canada from 2016 to 2017. Since then, he joined Huazhong University of Science and Technology to be a lecturer. His present research work involves quantum dot detectors and LEDs.

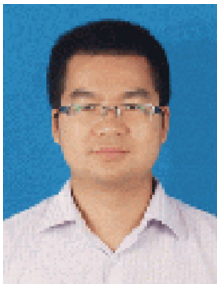

**Jiang Tang** received his Ph.D. degree from University of Toronto, Canada under the supervision of Prof. Edward H. Sargent in 2010 and undertook his postdoctoral research with Dr. David Mitzi at the IBM T. J. Watson Research Center from 2011 to 2012. Then, he became a full professor in Wuhan National Laboratory for Optoelectronics, Huazhong University of Science and Technology, China, since 2012. His research interests include luminescent materials and their applications, single crystals for X-ray detection, and antimony selenide thin film solar cells.